



## Synthesis, structure, magnetism, and hydrolase and catecholase activity of a new trinuclear copper(II) complex



Renata E.H.M.B. Osório<sup>a</sup>, Ademir Neves<sup>a,\*</sup>, Tiago Pacheco Camargo<sup>a</sup>, Sandro L. Mireski<sup>a</sup>, Adailton J. Bortoluzzi<sup>a</sup>, Eduardo E. Castellano<sup>b</sup>, Wolfgang Haase<sup>c</sup>, Zbigniew Tomkowicz<sup>d</sup>

<sup>a</sup> Laboratório de Bioinorgânica e Cristalografia (LABINC), Departamento de Química, Universidade Federal de Santa Catarina, 88040-900 Florianópolis, SC, Brazil

<sup>b</sup> Departamento de Física e Informática, Universidade de São Paulo, 13566-590 São Carlos, SP, Brazil

<sup>c</sup> Institut für Physikalische Chemie, Technische Universität Darmstadt, Petersenstraße 20, D-64287 Darmstadt, Germany

<sup>d</sup> Institute of Physics, Reymonta 4, Jagiellonian University, PL-30-059 Krakow, Poland

### ARTICLE INFO

#### Article history:

Received 29 April 2015

Received in revised form 25 June 2015

Accepted 25 June 2015

Available online 3 July 2015

#### Keywords:

Trinuclear Cu<sup>II</sup> complex

Hydrolase and catecholase activity

Catalytic promiscuity

### ABSTRACT

In this paper we report the synthesis of the new multidentate N,O-donor ligand H<sub>3</sub>L<sub>2</sub>pyald = (N,N'-bis-(2-pyridylmethyl)-(2-hydroxy-3-carbonyl-5-methylbenzyl)-1,3-propanediamine-2-ol) and its first trinuclear copper(II) complex, [Cu<sub>3</sub>(L<sub>2</sub>pyald)(μ-OAc)](ClO<sub>4</sub>)<sub>2</sub> (**1**). The structure of **1** was determined by X-ray crystallography and variable-temperature magnetic data in the temperature range of 4–300 K indicate weak antiferromagnetism ( $J_{1,2} \cong -1.0 \text{ cm}^{-1}$ ) between the Cu(1) and Cu(2) centers bridged by the μ-alkoxo and μ-acetate groups and weak ferromagnetic coupling ( $J_{1,3} = J_{2,3} \cong +4.0 \text{ cm}^{-1}$ ) involving the {Cu(1)(μ-phenoxo)Cu(3)} and {Cu(2)(μ-phenoxo)Cu(3)} structural units. Complex **1** shows significant catalytic activity towards the hydrolysis of the model substrate bis(2,4-dinitrophenyl)phosphate (2,4-BDNPP) as well as catechol oxidase activity since it efficiently catalyzes the oxidation of 3,5-di-*tert*-butylcatechol to 3,5-di-*tert*-butyl-*o*-benzoquinone by dioxygen. A comparison of the catalytic efficiency of **1** with its dinuclear parent complex [Cu<sub>2</sub>(H<sub>2</sub>bbppnol)(μ-OAc)]<sup>2+</sup> (H<sub>2</sub>bbppnol = N,N',N,N'-bis[(2-hydroxybenzyl)(2-methylpyridyl)]-1,3-propanediamine-2-ol) reveals that the hydrolase efficiency ( $k_{\text{cat}}/K_{\text{M}}$ ) is 12 times higher for **1**, while the catecholase efficiencies of these two compounds are similar.

© 2015 Elsevier B.V. All rights reserved.

### 1. Introduction

Multimetallic complexes are of great interest due to the special chemical and physical properties that result from the mutual interaction of two or more metal centers [1].

Trinuclear copper clusters with trigonal symmetry play a central role in the fundamental steps of biological catalysis by ubiquitous multicopper oxidases. The study of model complexes of these systems should not only provide a better understanding of the biological molecules but also assist in the development of new low-molecular-weight catalysts [2]. In fact, trinuclear copper(II) complexes with trigonal symmetry have attracted attention as magnetic materials and systems mimicking trinuclear metalloenzyme sites present in copper oxidases, such as ascorbate oxidase, ceruloplasmin and laccase [3]. One of the forms of the copper oxidases corresponds to an antiferromagnetically coupled trinuclear Cu(II) cluster [4].

On the other hand, the ability of a given natural or non-natural active site to catalyze more than one chemical transformation (catalytic promiscuity) constitutes a very important property of many enzymes, playing a natural role in evolution and, occasionally, in the biosynthesis of secondary metabolites [5]. While several enzymes displaying catalytic promiscuity have been the subject of recently reported investigations [6], there are few examples of synthetic analogues which exhibit such multifunctional activities [7–11].

In this paper we present a trinuclear copper(II) complex [Cu<sub>3</sub>(L<sub>2</sub>pyald)(μ-OAc)](ClO<sub>4</sub>)<sub>2</sub> – **1** with the novel symmetrical ligand H<sub>3</sub>L<sub>2</sub>pyald (Chart 1) which is able to stabilize a triangular Cu<sub>3</sub><sup>II</sup> structure containing Cu(II) centers with distinct coordination environments. It was found that complex **1** shows significant catalytic activity toward the hydrolysis of the activated substrate bis(2,4-dinitrophenyl)phosphate (2,4-BDNPP) as well as in the oxidation of 3,5-di-*tert*-butylcatechol (3,5-DTBC), thus indicating catalytic promiscuity.

\* Corresponding author. Tel.: +55 48 37216849; fax: +55 48 37216850.

E-mail address: [ademir.neves@ufsc.br](mailto:ademir.neves@ufsc.br) (A. Neves).

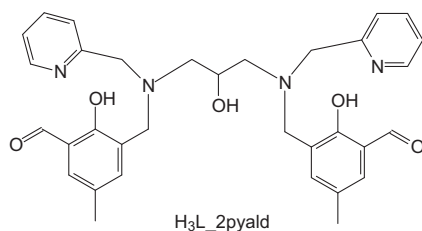


Chart 1. Ligand  $H_3L_{2pyald}$ .

## 2. Experimental

The materials 2,4-BDNPP = bis(2,4-dinitrophenyl)phosphate [12] and CMFF = 2-chloromethyl-4-methyl-6-formylphenol [13] were synthesized as previously described. Other reagents, materials, gases and solvents of analytical or spectroscopic grade were purchased from commercial sources and used without purification.

Elemental analysis (CHN) was performed on a Carlo Erba E-1110 analyzer. Electronic absorption spectra in the 300–1000 nm range were recorded on a UV–Vis Varian Cary 50 BIO spectrophotometer.  $^1H$  NMR analysis was carried out using a Bruker 200 MHz spectrometer with  $CDCl_3$  as the solvent, at room temperature. Chemical shifts were referenced to tetramethylsilane. Electrochemical measurements were carried out using a Bas Epsilon potentiostat/galvanostat. Cyclic voltammograms were obtained for the complex in acetonitrile solution containing 0.1 M tetrabutylammonium hexafluorophosphate as the supporting electrolyte under an argon atmosphere. The electrochemical cell employed was of a standard three-electrode configuration: glassy carbon electrode (working), platinum wire (counter), Ag/AgCl (reference). The  $Fc^+/Fc$  couple ( $E_{1/2} = 400$  mV versus NHE) was used as the internal standard [14].

Electrospray ionization mass spectrometry (ESI-MS) of **1** dissolved in an ultrapure acetonitrile solution (500 nM) was performed using an amaZon X Ion Trap MS instrument (Bruker Daltonics) with an ion spray source using electrospray ionization in positive-ion mode. The ion source condition was an ion spray voltage of 4500 V. Nitrogen was used as the nebulizing gas (20 psi) and curtain gas (10 psi). The samples were directly infused into the mass spectrometer at a flow rate of 180  $\mu$ L/h. The scan range was  $m/z$  200–3000. The simulated spectrum was calculated using the mMass software [15,16].

Magnetic data were obtained with a SQUID magnetometer using a slightly pressed (by hand) polycrystalline sample of complex **1**. Susceptibility data were measured in the temperature range of 4–300 K with a magnetic field of 1000 Oe. Magnetization data were obtained in the field range up to 5 T at a temperature of 2.0 K. Diamagnetic corrections were applied in the usual manner with the use of the tabulated Pascal's constants [17].

A green crystal of complex **1** with dimension of  $0.476 \times 0.42 \times 0.01$  mm<sup>3</sup> was selected from a crystalline sample and the crystallographic analysis was carried out with a Bruker KAPPA-CCD diffractometer at room temperature. Intensities were corrected for Lorentz and polarization effects. Gaussian absorption correction was also applied to all measured intensities with maximum and minimum transmission factors of 0.6092 and 0.9822, respectively. High values of  $R_{int}$  and  $R_{sigma}$  can be attributed to the shape and quality of the crystals. The structure was solved by direct methods and refined using the full-matrix least-squares on  $F^2$  method. All non-hydrogen atoms were refined with anisotropic displacement parameters. Hydrogen atoms bonded to C atoms were placed at their idealized positions using standard geometric

criteria. H atoms of the coordinated water molecule were not found from the Fourier difference map.

The hydrolase and catecholase-like activities of **1** were determined by measuring the hydrolysis reaction of the model substrate bis(2,4-dinitrophenyl)phosphate (2,4-BDNPP) and the oxidation of the substrate 3,5-di-*tert*-butylcatechol (3,5-DTBC), respectively, in a Varian Cary 50 BIO UV–Vis spectrophotometer fitted with a thermostated water-jacketed cell holder. The reactions were accompanied by monitoring the increase in the 2,4-dinitrophenolate characteristic absorption band at 400 nm ( $pH/\epsilon$  L mol<sup>-1</sup> cm<sup>-1</sup> = 3.5/2125; 4.0/3408; 4.5/7182; 5.0/10078; 5.5/11405; 6.0/12004; 6.5–10.0/12100) at 50 °C for the hydrolase-like activity [18] and the formation of 3,5-di-*tert*-butylquinone (3,5-DTBQ) at 400 nm ( $\epsilon = 1900$  M<sup>-1</sup>cm<sup>-1</sup>) for the catecholase-like activity at 25 °C. Less than 5% of the conversion of the substrate to the product was monitored and the data were treated using the initial rate method as previously described [9].

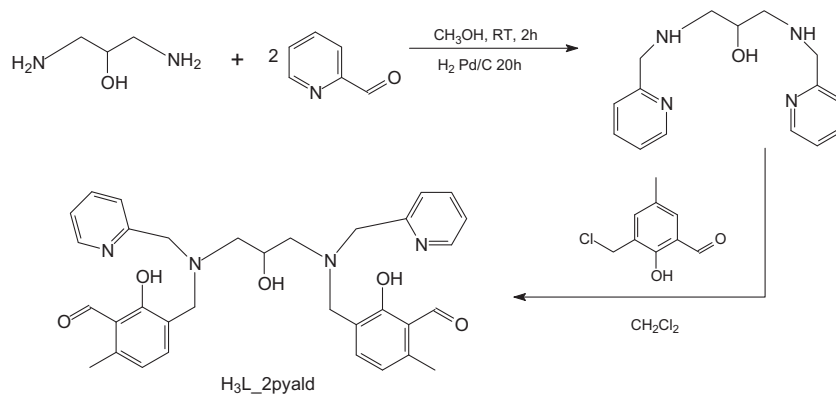
Synthesis of *N,N'*-(2-pyridylmethyl)-1,3-propanediamine-2-ol (2py): 4 mL of 2-pyridinecarboxaldehyde (40 mmol) in methanol was added slowly under continuous agitation, in an ice bath, to a solution containing 2.0 g (20 mmol) of 2-hydroxy-1,3-propanediamine in 30 mL of methanol. After 2 h of reaction the Schiff base was reduced overnight by catalytic hydrogenation using Pd/C (5%). The catalyst was filtered and the solvent removed under reduced pressure giving a yellow oil. Yield: 5.35 g (88%). The compound was obtained in high purity as confirmed by  $^1H$  NMR ( $CDCl_3$ ),  $\delta$  (ppm): 2.4–2.7 (4H); 3.3 (1H); 3.7–3.9 (4H); 6.9–7.1 (2H); 7.2–7.3 (2H); 7.4–7.6 (2H); 8.4 (2H).

Ligand  $H_3L_{2pyald}$  = (*N,N'*-bis-(2-pyridylmethyl)-(2-hydroxy-3-carbonyl-5-methylbenzyl)-1,3-propanediamine-2-ol): In a 125 mL round-bottom flask, 2.71 g (9.95 mmol) of 2py was dissolved in 30 mL of  $CH_2Cl_2$ . To this solution, 30 mL of a dichloromethane solution of 2-chloromethyl-4-methyl-6-formylphenol (3.68 g; 19.9 mmol) was added dropwise. The resulting mixture was allowed to react for 12 h with stirring at room temperature. The product was extracted with an aqueous solution of  $NaHCO_3$  (5  $\times$  50 mL). The organic layer was dried over  $Na_2SO_4$ , filtered and the solvent evaporated under reduced pressure, to give an oily product which was then purified by silica gel column chromatography with dichloromethane/methanol. Yield: 3.50 g (60%).  $^1H$  NMR ( $CDCl_3$ ),  $\delta$  (ppm): 2.2 (6H); 2.4–2.6 (4H); 3.6–4.0 (9H); 7.0–7.1 (4H); 7.2–7.3 (4H); 7.4–7.5 (2H); 8.4 (2H); 10.1 (2H). ESI-MS:  $m/z$  569.28 [M]<sup>+</sup>.

Synthesis of  $[Cu_3(L_{2pyald})(\mu-OAc)(ClO_4)_2 \cdot 1$ : To a yellow methanolic solution (20 mL) of 0.28 g of the ligand  $H_3L_{2pyald}$  (0.5 mmol), 0.30 g of  $Cu(OAc)_2 \cdot H_2O$  (1.5 mmol) previously dissolved in 10 mL of methanol was added dropwise, under stirring and the color immediately turned to dark green. Sodium perchlorate (1.5 mmol) was then added to the reaction mixture and after cooling the solution to room temperature a green microcrystalline precipitate was formed which was filtered off. After recrystallization in isopropanol/water (1:1) and slow evaporation of the solvents, green crystals suitable for X-ray analysis were isolated. Yield: 50%. Anal. Calc. for  $C_{35}H_{39}Cl_2Cu_3N_4O_{16}$ : C, 40.68; H, 3.80; N, 5.42. Found: C, 41.66; H, 4.34; N, 5.53%. ESI-MS:  $m/z$  912.00 [M]<sup>+</sup>.

## 3. Results and discussion

The ligand  $H_3L_{2pyald}$  was obtained with sufficient purity and yield for use in the synthesis of the trinuclear copper(II) complex. The reaction scheme for the preparation of the symmetrical ligand is depicted in Scheme 1.  $H_3L_{2pyald}$  was synthesized by typical procedures starting from the central skeleton 1,3-diaminepropane-2-ol condensed with pyridinecarboxaldehyde followed



Scheme 1. Synthesis of the ligand H<sub>3</sub>L<sub>2</sub>pyald.

by reduction with 5% Pd/C and alkylation with 2-chloromethyl-4-methyl-6-formylphenol [13].

Reaction of H<sub>3</sub>L<sub>2</sub>pyald in methanol with copper(II) acetate monohydrate (3 equiv.), in the presence of sodium perchlorate, affords the stable complex [Cu<sub>3</sub>(L<sub>2</sub>pyald)(μ-OAc)](ClO<sub>4</sub>)<sub>2</sub> – **1**. Recrystallization of **1** from a H<sub>2</sub>O/isopropyl alcohol solution afforded crystals suitable for X-ray crystallographic analysis.

The copper complex crystallizes as single green crystals that belong to the monoclinic crystal system, in the space group *P*2<sub>1</sub>/*c*. An ORTEP view of the trinuclear cation complex is shown in Fig. 1. The crystallographic data and the main bond distances/angles are given in Table S1 and Table 1, respectively. The resolution of the crystal structure revealed that **1** is composed of a trinuclear core in which one symmetrical ligand H<sub>3</sub>L<sub>2</sub>pyald is coordinated to two Cu(II) centers (Cu1 and Cu2) bridged by the alkoxy donor O atom of the ligand and by an exogenous acetate ion. The third Cu(II) center (Cu3) is tetra coordinated by four oxygen atoms of the ligand H<sub>3</sub>L<sub>2</sub>pyald.

The Cu1 center is pentacoordinated, showing a slightly distorted square pyramidal geometry ( $\tau = 0.18$ ), while the coordination around Cu2 is best described as a distorted octahedron with the phenolate (O41) and water (O1w) oxygen atoms bound in the axial positions. The equatorial plane of the two copper centers consists of one amine and one pyridine nitrogen and one acetate and one alkoxy oxygen atom. A deprotonated oxygen atom (O31) of the phenol group in the axial position completes the coordination sphere of the Cu1 center. The oxygen atoms of the phenolate groups interact weakly with the Cu1 and Cu2 centers since the observed Cu(II)–O distances are relatively long (Cu1–O31–2.565(4) Å and Cu2–O41–2.908(4) Å), as a result of the Jahn–Teller effect displayed by the Cu(II) ion. The coordination

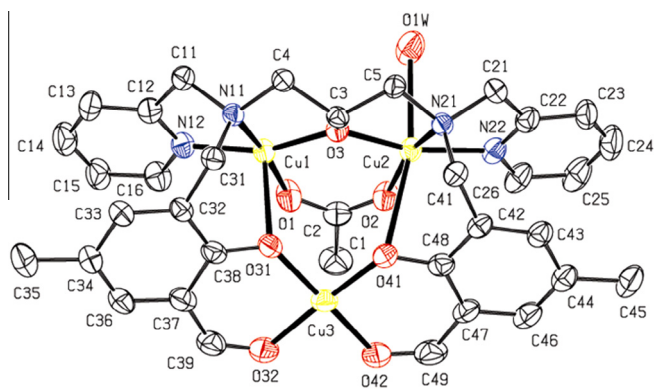


Fig. 1. ORTEP view of the cation complex [Cu<sub>3</sub>(L<sub>2</sub>pyald)(μ-OAc)](ClO<sub>4</sub>)<sub>2</sub> – **1**.

Table 1  
Main bond distances (Å) and angles (°) for complex **1**.

Cu1–O3	1.864(3)	Cu2–O41	2.908(4)
Cu1–O1	1.928(4)	Cu3–O41	1.886(4)
Cu1–N12	1.960(4)	Cu3–O31	1.888(4)
Cu1–N11	2.047(4)	Cu3–O42	1.921(4)
Cu1–O31	2.565(4)	Cu3–O32	1.951(4)
Cu2–O3	1.878(3)	Cu1–Cu2	3.3716(8)
Cu2–O2	1.937(3)	Cu2–Cu3	4.0535(9)
Cu2–N22	1.983(4)	Cu1–Cu3	3.7535(9)
Cu2–N21	2.049(4)	Cu2 O1W	2.485(5)
O3–Cu1–O1	98.11(15)	O3–Cu2–O2	98.84(15)
O3–Cu1–N12	160.88(16)	O3–Cu2–N22	164.80(16)
O1–Cu1–N12	94.31(17)	O2–Cu2–N22	94.67(17)
O3–Cu1–N11	85.42(14)	O3–Cu2–N21	85.37(14)
O1–Cu1–N11	171.88(18)	O2–Cu2–N21	163.14(17)
N12–Cu1–N11	84.21(16)	N22–Cu2–N21	83.67(17)
O3–Cu1–O31	89.45(13)	O3–Cu2–O1W	84.32(15)
O1–Cu1–O31	87.63(17)	O2–Cu2–O1W	103.67(19)
N12–Cu1–O31	105.59(15)	N22–Cu2–O1W	85.76(16)
N11–Cu1–O31	85.09(13)	N21–Cu2–O1W	92.96(17)
O41–Cu3–O31	89.39(15)	O3–Cu2–O41	80.09(12)
O41–Cu3–O42	93.60(17)	O2–Cu2–O41	83.36(14)
O31–Cu3–O42	174.4(2)	N22–Cu2–O41	108.52(14)
O41–Cu3–O32	177.54(17)	N21–Cu2–O41	81.30(13)
O31–Cu3–O32	93.05(17)	O1W–Cu2–O41	163.75(13)
O42–Cu3–O32	84.01(19)	Cu1–O3–Cu2	128.58(16)
Cu3–O41–Cu2	113.7516	Cu3–O31–Cu1	114.04(16)

sphere of the Cu3 center is composed of four oxygen atoms, provided by two endogenous phenolates (O31 and O41) and two aldehyde oxygen atoms of the ligand H<sub>3</sub>L<sub>2</sub>pyald (O32 and O42). The O–Cu3–O bond angles close to 90° and 180° found for the Cu3 center are in agreement with a square planar geometry.

Fig. 2 shows the magnetic data obtained for **1**. They are presented in the form of the product of susceptibility multiplied by temperature ( $\chi T$ ) plotted as a function of the temperature *T* and of the magnetization *M* plotted as a function of the field *H/T*. The former dependence was recorded in a field of 1000 Oe and the latter at temperatures of 2.0, 4.5 and 10 K. It can be observed that the room temperature value for  $\chi T$  is 1.48 emu/mol K, which may be compared with the predicted value for three free 1/2 spins of 1.125 emu/mol K (for *g* = 2). It can also be seen in Fig. 2 that the *M* value in the highest available field of 5 T at a temperature of 2 K is 2.48 μ<sub>B</sub>, which may be compared with the value of 2.8 μ<sub>B</sub> expected for three free 1/2 spins (see the dot-dashed Brillouin curve in Fig. 2). Magnetization curves plotted as a function of *H/T* superimpose above 4.5 K, indicating simple paramagnetic behavior above this temperature.

The lower value for the high field-low temperature magnetization may be caused by zero field splitting due to the antisymmetric

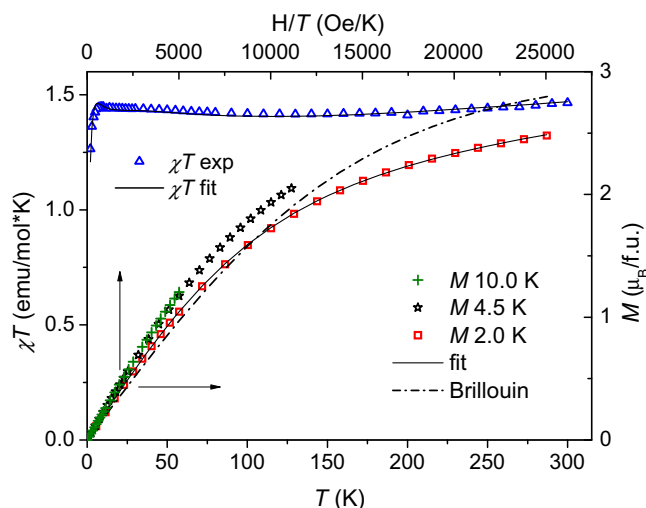


**Fig. 2.** Temperature dependence of the  $\chi T$  product measured in a field of 1000 Oe and  $H/T$  dependence of magnetization  $M$  measured at 2, 4.5 and 10 K for the complex  $[\text{Cu}_3(\text{L}_2\text{pyald})(\mu\text{-OAc})(\text{ClO}_4)_2 - 1]$ . Solid lines are fits. Dash-dot line is the Brillouin function plotted for three uncoupled  $1/2$  spins.

and anisotropic exchange [19,20]. For the description of the magnetic behavior we used the Hamiltonian of the following form

$$H = -2 \sum_{i < j}^3 [\vec{S}_i \cdot \vec{J}_{ij} \cdot \vec{S}_j + \vec{d}_{ij} \cdot (\vec{S}_i \times \vec{S}_j)] + \mu_B \sum_{i=1}^3 (\vec{S}_i \cdot \vec{g}_i) \cdot \vec{H},$$

$$\text{where } \vec{J}_{ij} = \begin{bmatrix} J_{ijx} & 0 & 0 \\ 0 & J_{ijy} & 0 \\ 0 & 0 & J_{ijz} \end{bmatrix} \text{ and } \vec{d}_{ij} = \begin{bmatrix} d_{ijx} \\ d_{ijy} \\ d_{ijz} \end{bmatrix}.$$

In the above equations  $J_{ijx}, J_{ijy}, J_{ijz}$  are the components of the isotropic/anisotropic exchange when all these components are equal/not equal, respectively.  $d_{ijx}, d_{ijy}, d_{ijz}$  are components of the antisymmetric exchange.

To obtain the exchange parameters, the simultaneous fitting of the values for the  $\chi T$  product and the magnetization data was performed using the PHI software [21]. The trials were initially carried out with the lowest possible number of parameters, i.e., assuming that only the  $J_{12}$  interaction differs from zero, which was based on the relatively long distances of Cu2–O31 (2.908 Å) and Cu1–O41 (2.565 Å) in comparison with Cu1–O3 (1.877 Å) or Cu2–O3 (1.864 Å). The decrease in the  $M$  values observed in high fields at 2 K was not reproduced.

In the second stage, the  $J_{23}$  interaction was taken into account. To obtain a good fit it was necessary to assume the presence of anisotropy for both the  $J_{12}$  and  $J_{23}$  interactions and antisymmetric exchange for at least the  $J_{23}$  interaction. However, due to the large number of parameters no unambiguous solution was obtained, even though we used all three sets of magnetization data (2, 4.5 and 10 K) during each fitting. We could only confirm, in agreement with expectations, that the average value for  $J_{12}$  is negative, of the order of  $-1 \text{ cm}^{-1}$ , and the average value for  $J_{23}$  is positive (ferromagnetic coupling), of the order of  $4 \text{ cm}^{-1}$ . The exact values for the parameters from one exemplary fit are  $(J_{12x}, J_{12y}, J_{12z}) = (-3.7, -3.7, 3.4) \text{ cm}^{-1}$ ;  $(d_{ijx}, d_{ijy}, d_{ijz}) = (-1.5, -1.5, 2.8) \text{ cm}^{-1}$ ;  $(J_{23x}, J_{23y}, J_{23z}) = (2.8, 0.2, 8.5) \text{ cm}^{-1}$ ;  $(d_{23x}, d_{23y}, d_{23z})$  fixed at  $(0, 0, 0)$ ;  $g_1 = g_2 = 2.24, g_3 = 2.16$ .

From the X-ray structure of **1** it can be concluded that the geometries around Cu(1) and Cu(2) are, respectively, distorted square pyramidal and octahedral with significant tetragonal elongation toward the Cu1–O31 and Cu2–O41 bonds. Therefore, in both copper centers, the dominant magnetic orbital appears to be the

$d_{x-y}^2$  orbital (Cu1–O3 = 1.864(3) Å and Cu2–O3 = 1.878(3) Å) and thus the unpaired electrons can interact with the  $\mu$ -alkoxo group giving rise to weak antiferromagnetism ( $J_{1,2} \cong -1.0 \text{ cm}^{-1}$ ). On the other hand, in **1**, Cu3 lies in a slightly distorted square planar geometry as can be observed from the bond angles around this center and thus the unpaired electron is also in the  $d_{xy}^2$  magnetic orbital. However, in this case, this orbital is orthogonally oriented in relation to the  $d_{xy}^2$  orbitals of the Cu1 and Cu2 centers, leading to weak ferromagnetic coupling ( $J_{1,3} = J_{2,3} \cong +4.0 \text{ cm}^{-1}$ ) between the Cu3 and Cu1/Cu2 centers. For comparison, the weak antiferromagnetism ( $J = -1.0 \text{ cm}^{-1}$ ) between Cu(1) and Cu(2) falls in the range of  $J$  values observed for many  $\text{Cu}(\mu\text{-alkoxo})(\mu\text{-Acetate})\text{Cu}$  complexes reported in the literature [22,23]. On the other hand, the weak ferromagnetic exchange ( $J_{1,3} = J_{2,3} \cong +4.0 \text{ cm}^{-1}$ ) between the Cu(3) and Cu(1)/Cu(2) centers are in agreement with the ferromagnetic coupling observed for open type dinuclear Cu(II) complexes with a single  $\mu$ -phenoxo bridging ligand [24].

The redox properties of the complex  $[\text{Cu}_3(\text{L}_2\text{pyald})(\mu\text{-OAc})(\text{ClO}_4)_2]$  are given in Fig. S1 (see Supplementary Material) and were investigated in acetonitrile by cyclic voltammetry which revealed the presence of three irreversible waves with  $\text{Fc}^+/\text{Fc}$  as the internal standard. The first process at  $-360 \text{ mV}$  ( $E_{pc}$ ) versus NHE is assigned to the one-electron reduction of  $\text{Cu}_3^{\text{II}}/\text{Cu}_2^{\text{II}}\text{Cu}^{\text{I}}$ , while the waves at  $-580$  and  $-980 \text{ mV}$  versus NHE can be attributed to the couples  $\text{Cu}_2^{\text{II}}\text{Cu}^{\text{I}}/\text{Cu}^{\text{II}}\text{Cu}_2^{\text{I}}$  and  $\text{Cu}^{\text{II}}\text{Cu}_2^{\text{I}}/3\text{Cu}_2^{\text{I}}$ , respectively. In fact, these values are in good agreement with the reduction potentials observed for dinuclear copper(II) complexes containing a  $\mu$ -alkoxo bridge and phenolate/pyridine ligands [7,9,10].

The electronic spectrum of **1** (Fig. S2) in methanolic solution and in the solid state exhibits transitions at  $\lambda_{\text{max}} = 662 \text{ nm}$  ( $\epsilon = 185 \text{ L mol}^{-1} \text{ cm}^{-1}$ ) and  $\lambda_{\text{max}} = 510 \text{ nm}$  ( $\epsilon = 110 \text{ L mol}^{-1} \text{ cm}^{-1}$ ) typical of  $\text{Cu}^{\text{II}}$  d-d transitions and one band at  $382 \text{ nm}$  ( $\epsilon = 4934 \text{ L mol}^{-1} \text{ cm}^{-1}$ ), which can be attributed to a ligand-to-metal charge transfer between the phenolates and copper centers, in agreement with the X-ray structure characterization. In acetonitrile solution, an additional shoulder was observed at  $330 \text{ nm}$ , possibly associated with an intraligand transition involving phenolate/pyridine ligands. In fact, these results together with the ESI-MS spectrum (Fig. S3), which shows a peak at  $m/z = 912.00$  assigned to the  $[\text{Cu}_3(\text{L}_2\text{pyald})(\mu\text{-OAc})(\text{ClO}_4)]^+$  species, suggest that the coordination of the ligand  $\text{L}_2\text{pyald}$  around the  $\text{Cu}^{\text{II}}$  centers is maintained when the complex is dissolved under these experimental conditions.

Kinetic experiments were carried out to assess the ability of complex **1** to hydrolyze the substrate bis(2,4-dinitrophenyl)phosphate (2,4-BDPP). In order to determine the optimum pH, the dependence of the reaction rate was evaluated in  $\text{CH}_3\text{CN}:\text{H}_2\text{O}$  (1:1) within the pH range of 4.00–10.00. As can be seen in Fig. S4, the optimum pH is around 8.0 and sigmoidal fitting of the initial rate ( $V_0$ ) versus pH curve in the pH range of 4.0–8.0 reveals a kinetic  $\text{pK}_a$  value of  $\sim 6.9$ , which can be attributed to the deprotonation of a  $\text{Cu}^{\text{II}}$ -bound water molecule to generate the initiating nucleophile [9,25]. It is important to note that under these experimental conditions dissociation of the acetate bridge with replacement by two water molecules is expected, as previously reported in the literature [9]. Thus, the small decrease in reactivity at  $\text{pH} > 8.0$  (see Fig. S4) most probably originates from the formation of a further  $\text{Cu}^{\text{II}}\text{-OH}$  group in which the leaving tendency of the  $\text{OH}^-$  ion is lower, even though a more concentrated  $\text{OH}^-$  solution can increase the spontaneous hydrolysis [13].

The dependence of the reaction rate on the concentration of the diester 2,4-BDPP by complex **1** was investigated at  $\text{pH} 8.0$ , revealing saturation behavior with a higher concentration of the substrate (Fig. 3). The data were treated using the Michaelis–Menten model and the parameters  $V_{\text{max}} = 2.54 \times 10^{-8} \text{ mol L}^{-1} \text{ s}^{-1}$ ,  $K_M = 2.61 \times 10^{-3} \text{ mol L}^{-1}$  and  $k_{\text{cat}} = 9.76 \times 10^{-4} \text{ s}^{-1}$  were obtained

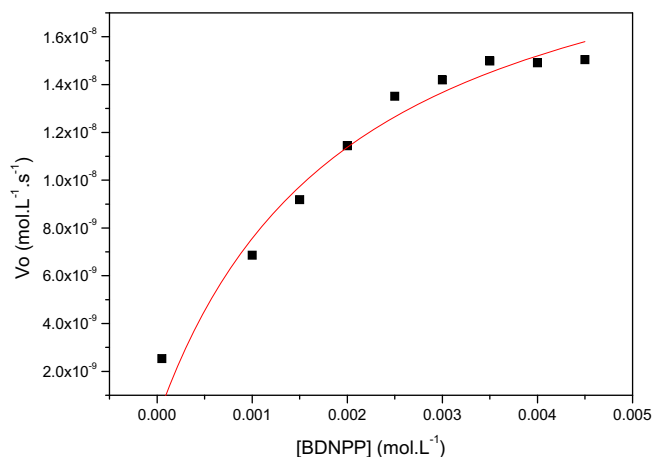


**Fig. 3.** Dependence of the initial rate on the 2,4-BDNPP concentration for the hydrolysis reaction catalyzed by complex **1**. Conditions: solution 1:1 CH<sub>3</sub>CN/H<sub>2</sub>O; [complex] =  $2.6 \times 10^{-5}$  mol L<sup>-1</sup>; [buffer] = 0.05 mol L<sup>-1</sup>; HEPES (pH 8.0); I = 0.05 mol L<sup>-1</sup> LiClO<sub>4</sub>; [2,4-BDNPP] =  $(0.5\text{--}8.0) \times 10^{-3}$  mol L<sup>-1</sup> at 50 °C.

from a nonlinear least-squares fit. A comparison of these kinetic parameters with those previously reported for the dinuclear [Cu<sub>2</sub>(H<sub>2</sub>bbppnol)(μ-OAc)](ClO<sub>4</sub>)<sub>2</sub> complex (H<sub>2</sub>bbppnol corresponds to the L<sub>2</sub>pyald ligand without the carbonyl function) reveals that **1** is about 12 times more efficient ( $E = k_{\text{cat}}/K_M = 0.37$  L mol<sup>-1</sup> s<sup>-1</sup>) than the dinuclear complex [26]. Indeed the higher catalytic efficiency of **1** is a direct consequence of the catalytic constant  $k_{\text{cat}}$  which is approximately 30 times the value of  $3.4 \times 10^{-5}$  s<sup>-1</sup> observed for the dinuclear complex. This is most probably due to the higher nucleophilic reactivity of the Cu<sup>II</sup>-bound OH<sup>-</sup> group in **1** ( $pK_a = 6.9$  in **1** versus 5.7 in [Cu<sub>2</sub>(H<sub>2</sub>bbppnol)(μ-OAc)]<sup>2+</sup>). In addition, this  $k_{\text{cat}}$  corresponds to an acceleration of ~4000 times with respect to the uncatalyzed reaction [12].

In order to assess the possible hydrolysis of the monoester 2,4-dinitrophenylphosphate (2,4-DNPP), one of the products formed from the hydrolysis of the diester 2,4-BDNPP, the stoichiometric reaction between complex **1** and the substrate 2,4-BDNPP was monitored. It was observed that over 3 days at 50 °C, only 1.2 equiv. of 2,4-dinitrophenolate is released, which indicates only diesterase activity for [Cu<sub>3</sub>(L<sub>2</sub>pyald)(μ-OAc)](ClO<sub>4</sub>)<sub>2</sub>. Furthermore, a hydrolysis reaction of 2,4-BDNPP ( $2.0 \times 10^{-3}$  mol L<sup>-1</sup>) promoted by complex **1** at 445 nm, pH 8.0 and 50 °C revealed that over 24 h the complex was able to hydrolyze 3 molecules of substrate, indicating that the active species is regenerated. The measured deuterium kinetic isotope effect  $k_H/k_D$  of 1.40 suggests that no proton transfer is involved in the rate-limiting step and thus supports an intramolecular nucleophilic attack of a terminal Cu-bound hydroxide on the phosphodiester which is monodentate bonded to the adjacent Cu<sup>II</sup> center in **1** [13,18].

The catecholase-like activity of the trinuclear copper(II) complex was determined by the catalytic oxidation of 3,5 di-*tert*-butylcatechol (3,5-DTBC). The pH dependence of the catalytic activity between pH 5.50 and 9.00 shows a sigmoidal-shaped profile (Fig. S5) and reveals an optimum value of pH 9.0. This value is ~1.0 pH unit higher than that found for the dinuclear [Cu<sub>2</sub>(H<sub>2</sub>bbppnol)(μ-OAc)]<sup>2+</sup> complex [26], again in agreement with the lower Lewis acidity of the Cu<sup>II</sup> centers within the Cu(1)(μ-alkoxo)Cu(2) unit in **1**. To take into account the auto-oxidation of the substrate, the same solution without the catalyst was used as an internal reference. Saturation kinetics were obtained at the pH value (9.0) where complex **1** showed greatest activity in the 3,5-DTBC oxidation. The graph of initial rates ( $V_0$ ) versus 3,5-DTBC concentrations shows a saturation profile (Fig. 4). Applying the

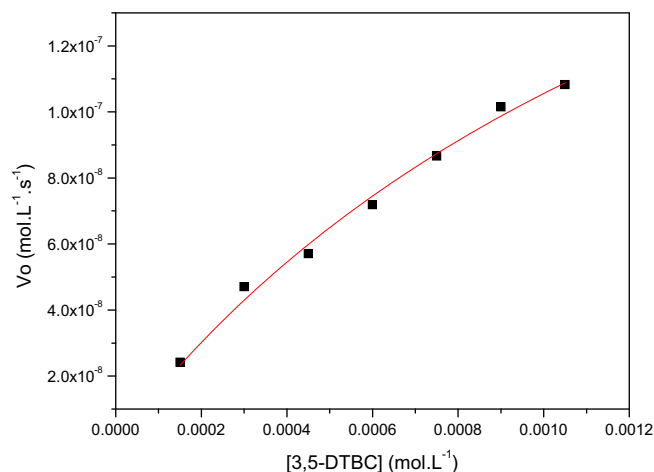


**Fig. 4.** Dependence of the reaction rates on the 3,5-DTBC concentration for the oxidation reaction catalyzed by complex **1** in a methanol/water solution. Conditions: [complex] =  $1.2 \times 10^{-5}$  mol L<sup>-1</sup>; [buffer] =  $3.0 \times 10^{-2}$  mol L<sup>-1</sup>; HEPES (pH 9.0); [3,5-DTBC] =  $(1.5\text{--}12.0) \times 10^{-4}$  mol L<sup>-1</sup> at 25 °C.

Michaelis–Menten approach it is possible to characterize the kinetic behavior using the parameters:  $k_{\text{cat}} = 0.0223$  s<sup>-1</sup>,  $K_M = 1.51 \times 10^{-3}$  mol L<sup>-1</sup> and  $k_{\text{cat}}/K_M = 14.86$  M<sup>-1</sup> s<sup>-1</sup>. A comparison with the [Cu<sub>2</sub>(H<sub>2</sub>bbppnol)(μ-OAc)]<sup>2+</sup> complex [27] reveals that the catalytic constant  $k_{\text{cat}}$  is approximately 3 times higher for **1** while  $K_{\text{ass}} \cong 1/K_M$  is almost double for the dinuclear complex, resulting in similar catalytic efficiencies ( $k_{\text{cat}}/K_M$ ) for the two systems.

Finally, accumulation of H<sub>2</sub>O<sub>2</sub> during turnover was confirmed by means of the molybdate-accelerated I<sup>-3</sup> assay, which indicates that reoxidation of the copper(I) species back to the active copper(II) species occurs with a 1:1 (O<sub>2</sub>:3,5-DTBC) stoichiometry and the concomitant formation of hydrogen peroxide. Thus, it can be concluded that **1** and [Cu<sub>2</sub>(H<sub>2</sub>bbppnol)(μ-OAc)]<sup>2+</sup> most probably catalyze the oxidation of 3,5-DTBC through a similar mechanism [27]. In brief, bidentate binding of the diphenol substrate is followed by an intramolecular electron-transfer reaction with concomitant release of the *o*-quinone as the rate-determining step. In the presence of dioxygen, the Cu<sup>I</sup>Cu<sup>I</sup> center is immediately oxidized back to the original active site with the formation of H<sub>2</sub>O<sub>2</sub>, completing the catalytic cycle.

In summary, we synthesized and fully characterized the new trinuclear Cu<sup>II</sup> complex [Cu<sub>3</sub>(L<sub>2</sub>pyald)(μ-OAc)](ClO<sub>4</sub>)<sub>2</sub> (**1**) which has a dinuclear Cu(1)(μ-alkoxo)Cu(2) core similar to that observed for its dinuclear parent complex [Cu<sub>2</sub>(H<sub>2</sub>bbppnol)(μ-OAc)]<sup>2+</sup> [23,25]. The complex displays interesting magnetic properties which reveal antiferromagnetism between the Cu(1) and Cu(2) centers within the Cu(1)(μ-alkoxo)Cu(2) unit and ferromagnetism between the Cu(1)Cu(3) and Cu(2)Cu(3) centers, in good agreement with the X-ray structural data. Finally, **1** shows significant catecholase activity and is also able to cleave the phosphate diester bis(2,4-dinitrophenyl)phosphate with a catalytic activity ( $k_{\text{cat}}$ ) 30 times higher than that of the dinuclear [Cu<sub>2</sub>(H<sub>2</sub>bbppnol)(μ-OAc)]<sup>2+</sup> complex, due to the higher nucleophilic reactivity of the Cu<sup>II</sup>-bound OH<sup>-</sup> group in **1**.

## Acknowledgements

The authors are grateful for grants awarded to support this research from CNPq, FINEP, CAPES-STINT and INCT-Catálise (Brazil).

## Appendix A. Supplementary material

Crystallographic data for the structure reported in this paper (complex **1**) have been deposited with the Cambridge Crystallographic Data Centre as supplementary publication no. CCDC 1049454. Copies of the data can be obtained free of charge from the CCDC (12 Union Road, Cambridge CB2 1EZ, UK; tel: (+44) 1223-336-408; fax: (+44) 1223-336-003; e-mail: deposit@ccdc.cam.ac.uk; website [www.ccdc.cam.ac.uk](http://www.ccdc.cam.ac.uk)). Supplementary data associated with this article can be found, in the online version, at <http://dx.doi.org/10.1016/j.ica.2015.06.023>.

## References

- [1] S.L. Ma, W.X. Zhu, S. Gao, Q.L. Guo, M.Q. Xu, *Eur. J. Inorg. Chem.* (2004) 1311.
- [2] P. Mateus, R. Delgado, F. Lloret, J. Cano, P. Brandão, V. Félix, *Chem. Eur. J.* 17 (2011) 11193.
- [3] A. Messerschmidt, R. Huber, *Eur. J. Biochem.* 187 (1990) 341.
- [4] M.J. Kobyłka, J. Janczak, T. Lis, T. Kowalik-Jankowska, J. Klak, M. Pietruska, J. Lisowski, *Dalton Trans.* 41 (2012) 1503.
- [5] P.J. O'Brien, *Chem. Rev.* 106 (2006) 720.
- [6] R.J. Kazlauskas, *Curr. Opin. Chem. Biol.* 2 (2005) 195.
- [7] N.A. Rey, A. Neves, A.J. Bortoluzzi, C.T. Pich, H. Terenzi, *Inorg. Chem.* 46 (2007) 348.
- [8] K.M. Deck, T.A. Tseng, J.N. Burstyn, *Inorg. Chem.* 41 (2002) 669.
- [9] R.E.H.M.B. Osório, R.A. Peralta, A.J. Bortoluzzi, V.R. de Almeida, B. Szpoganicz, F.L. Fischer, H. Terenzi, A.S. Mangrich, K.M. Mantovani, D.E.C. Ferreira, W.R. Rocha, W. Haase, Z. Tomkowicz, A. dos Anjos, A. Neves, *Inorg. Chem.* 51 (2012) 1569.
- [10] A. Neves, A.J. Bortoluzzi, R. Jovito, R.A. Peralta, B. de Souza, B. Szpoganicz, A.C. Youssef, H. Terenzi, P.C. Severino, F.L. Fischer, G. Schenk, M.J. Riley, S.J. Smith, L.R. Gahan, *J. Braz. Chem. Soc.* 21 (2010) 1201.
- [11] M.C.B. Oliveira, D. Mazera, M. Scarpellini, P.C. Severino, A. Neves, H. Terenzi, *Inorg. Chem.* 48 (2009) 2711.
- [12] C.A. Bunton, S.J. Farber, *J. Org. Chem.* 34 (1969) 767.
- [13] P. Karsten, A. Neves, A.J. Bortoluzzi, M. Lanznaster, V. Drago, *Inorg. Chem.* 41 (2002) 4624.
- [14] R.R. Gagne, C.A. Koval, G.C. Lisensky, *Inorg. Chem.* 19 (1980) 2854.
- [15] M. Strohal, M. Hassman, B. Košata, M. Kodíček, *Rapid Commun. Mass Spectrom.* 22 (2008) 905.
- [16] M. Strohal, D. Kavan, P. Novák, M. Volný, *Anal. Chem.* 82 (2010) 4648.
- [17] C.J. O'Connor, *Prog. Inorg. Chem.* 29 (1982) 203.
- [18] R.A. Peralta, A.J. Bortoluzzi, B. de Souza, R. Jovito, F.R. Xavier, R.A.A. Couto, A. Casellato, F. Nome, A. Dick, L.R. Gahan, G. Schenk, G.R. Hanson, F.C.S. de Paula, E.C. Pereira-Maia, S.P. Machado, P.C. Severino, C. Pich, T. Bortolotto, H. Terenzi, E.E. Castellano, A. Neves, M.J. Riley, *Inorg. Chem.* 49 (2010) 11421.
- [19] J. Yoon, L.M. Mirica, T.D.P. Stack, E. Solomon, *J. Am. Chem. Soc.* 126 (2004) 12586.
- [20] S. Ferrer, F. Lloret, E. Pardo, J.M. Clemente-Juan, M. Liu-González, S. García-Granda, *Inorg. Chem.* 51 (2012) 985.
- [21] N.F. Chilton, R.P. Anderson, L.D. Turner, A. Soncini, K.S. Murray, *J. Comput. Chem.* 34 (2013) 1164.
- [22] C.H. Weng, S.C. Cheng, H.M. Wei, H.H. Wei, C.J. Lee, *Inorg. Chim. Acta* 359 (2006) 2029.
- [23] A. Neves, L.M. Rossi, I. Vencato, V. Drago, W. Haase, R. Werner, *Inorg. Chim. Acta* 281 (1998) 111.
- [24] R.C. Holz, J.M. Brink, F.T. Gobena, C.J. O'Connor, *Inorg. Chem.* 33 (1994) 6086.
- [25] R.A. Peralta, A. Neves, A.J. Bortoluzzi, A. dos Anjos, F.R. Xavier, B. Szpoganicz, H. Terenzi, M.C.B. Oliveira, E.E. Castellano, G.R. Friedermann, A.S. Mangrich, M.A. Novak, *J. Inorg. Biochem.* 100 (2006) 992.
- [26] L.M. Rossi, A. Neves, A.J. Bortoluzzi, R. Hörner, B. Szpoganicz, H. Terenzi, A.S. Mangrich, E.C. Pereira-Maia, E.E. Castellano, W. Haase, *Inorg. Chim. Acta* 358 (2005) 1807.
- [27] A. Neves, L.M. Rossi, A.J. Bortoluzzi, B. Szpoganicz, C. Wiezbicki, E. Schwingel, W. Haase, S. Ostrovsky, *Inorg. Chem.* 41 (2002) 1788.